

Comments on "Scattering of Inertial Waves by an Ocean Front"

P. KLEIN AND A. M. TREGUIER

Laboratoire de Physique des Océans, IFREMER, Plouzané, France

11 May 1994 and 14 July 1994

1. Introduction

Rubenstein and Roberts (1986, hereafter RR86) have studied the scattering of inertial waves by a geostrophic jet. The most remarkable effect of the jet is to concentrate near-inertial energy in the negative vorticity region. This effect is due to the horizontal dispersion of near-inertial waves. It is demonstrated by RR86 using a stratified linearized model. A similar result has been obtained by Kunze (1985) using a ray-tracing approach and has been confirmed by observations (Kunze and Stanford 1984).

Another result of RR86 concerns the mixed layer depth variations. Their Figs. 3 and 8 show a systematic downwelling in the negative vorticity region of the jet and systematic upwelling in the positive vorticity region. Although large upwellings and downwellings occur in the presence of a wind stress perpendicular to the front (Niiler 1969), it is not clear how such systematic effects can result from unforced inertial oscillations. RR86 find this behavior of the mixed layer depth in a shallow-water model where horizontal dispersion is neglected (their Fig. 3) and therefore suggest it is due to the nonlinearity of the mass equation.

Our failure to reproduce the results of RR86 with a fully nonlinear shallow-water model led us to investigate more carefully the role of nonlinear terms, using both direct numerical simulation and asymptotic analysis. In the present note we show that the systematic upwellings and downwellings are spurious effects due to the neglect of some (but not all) nonlinear terms in RR86's mixed layer equations.

2. Inertial oscillations in the mixed layer in the presence of a geostrophic jet

As in RR86 we assume a barotropic geostrophic jet, independent of y and steady. Effects of the jet velocity $V(x)$ on the mixed layer dynamics are assessed using a $1\frac{1}{2}$ -layer model, which consists of a surface mixed layer (with velocities $\tilde{u} = u$, $\tilde{v} = v + V$) of depth h capping an abyssal layer where the only motion con-

sidered is the jet velocity. Since the only spatial heterogeneity comes from the geostrophic jet $V(x)$, the variations in y are assumed negligible compared with the x derivatives. The resulting equations for u , v , and h are

$$\frac{\partial u}{\partial t} - fv + u \frac{\partial u}{\partial x} = -g' \frac{\partial h}{\partial x} + \nu \frac{\partial^2 u}{\partial x^2} \quad (1)$$

$$\frac{\partial v}{\partial t} + (f + \zeta)u + u \frac{\partial v}{\partial x} = \nu \frac{\partial^2 v}{\partial x^2} \quad (2)$$

$$\frac{\partial h}{\partial t} + \frac{\partial hu}{\partial x} = 0, \quad (3)$$

with $f = 10^{-4} \text{ s}^{-1}$ the Coriolis parameter, g the gravitational acceleration, $g' = g \Delta \rho / \rho$ the reduced gravity, $\zeta = \partial V / \partial x$ the jet vorticity, and ν the friction coefficient.

In the numerical experiments $V(x)$ is a Gaussian:

$$V(x) = V_0 e^{-(x^2/2\lambda^2)} \quad (4)$$

with $V_0 = 0.2 \text{ m s}^{-1}$ and $\lambda = 20 \text{ km}$. The Gaussian is preferred to the cosine shape used by RR86 because in their case the vorticity gradients are infinite at the jet's edges. This generates numerical noise unless the solutions are viscous enough (which was the case in RR86 due to the low spatial resolution). The results presented below are qualitatively independent of the details of the jet shape.

Numerical solutions are obtained using standard finite-difference methods on a staggered grid. Viscosity is small ($\nu = 10 \text{ m}^2 \text{ s}^{-1}$). The domain is periodic in x , 300 km wide, and the grid size is 1 km. We have verified that the solutions do not change when the grid is refined. As in RR86, initial conditions are $h_i = 50 \text{ m}$, $u_i = 0$, and $v_i = 0.2 \text{ m s}^{-1}$ at $t = 0$. The nonzero inertial energy ($v_i^2/2$) corresponds to the energy that would be forced by a spatially uniform wind stress blowing during half an inertial period.

The case without horizontal dispersion ($g' = 0$) is considered first. Linear solutions have been discussed by Klein and Treguier (1993, hereafter KT93). The linear system is obtained from (1)–(3) by dropping the nonlinear advection from the momentum equations and linearizing the mass equation as

Corresponding author address: Dr. Patrice Klein, UM/LPO, IFREMER, Centre de Brest, B.P. 70, Plouzané 29280, France.

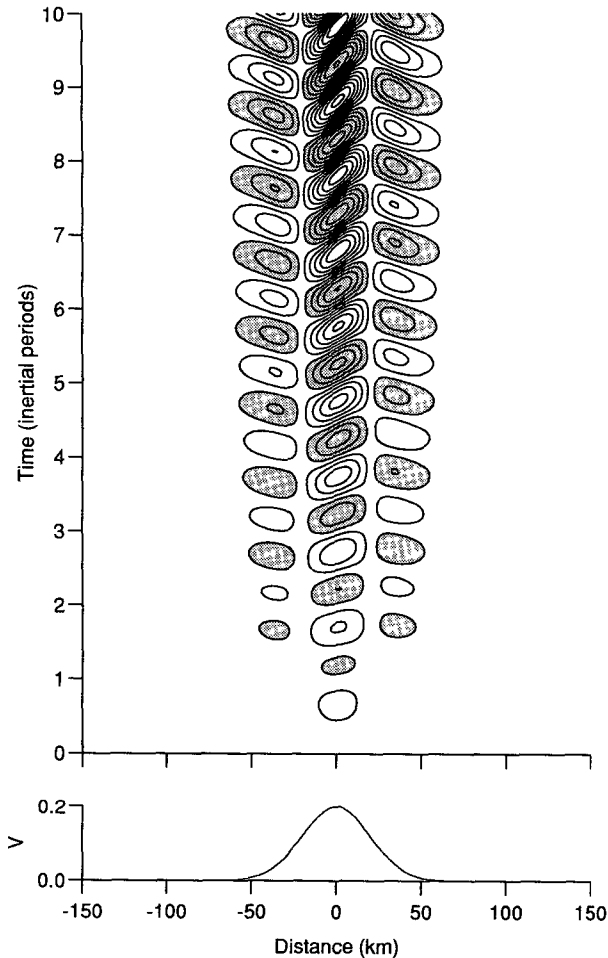


FIG. 1. Time-longitude plot of the mixed layer depth perturbation ($h^* = h - h_i$ with $h_i = 50$ m) for the linear equations, with $g' = 0$ and $\nu = 10 \text{ m}^2 \text{ s}^{-1}$. Contour interval is 2 m, from -13 to 13 m. Positive values (downwelling) are shaded. The velocity of the geostrophic jet (m s^{-1}) is indicated below.

$$\frac{\partial h}{\partial t} + h_i \frac{\partial u}{\partial x} = 0. \quad (5)$$

A time-longitude plot of the mixed layer depth perturbation is shown in Fig. 1 for such a linear solution. Its characteristics can be summarized as follows. At first, the inertial oscillations have no spatial variability and the mixed layer depth remains uniform. However, the frequency ω of the oscillations is modified by the jet vorticity ζ . The x dependency of the frequency causes a growing spatial variability, characterized by a pseudowavenumber $k = -t\partial\omega/\partial x$ (RR86). This growing variability produces the growing oscillations of the mixed layer depth apparent in Fig. 1; after 10 inertial periods the maximum downwelling amplitude is 13 m.

RR86 use the linear form of the momentum equations but use the nonlinear form of the mass equation

(3). The mixed layer depth evolution is quite different in that case (Fig. 2), with a systematic upwelling in the positive vorticity region and large downwelling in the negative vorticity region, reaching a maximum of 52 m after 10 inertial periods. RR86 attribute this effect to the nonlinear advection term in (3).

However, the solution of the fully nonlinear system (1)–(3) is very close to the linear solution (Fig. 3) and does not display any systematic upwelling or downwelling. This surprising result motivated a more careful analysis of nonlinear effects, using an asymptotic analysis.

3. Asymptotic analysis

Let us nondimensionalize the system (1)–(3), with $g' = \nu = 0$, using the jet scale λ as a lengthscale, $1/f$ as a timescale, v_i as a velocity scale, and h_i as a depth scale. The parameter $\epsilon = v_i/f\lambda$ is assumed to be small ($\epsilon \ll 1$). Then (1)–(3) become (nondimensional variables are noted by an asterisk)

$$\frac{\partial u^*}{\partial t^*} - v^* + \epsilon u^* \frac{\partial u^*}{\partial x^*} = 0 \quad (6)$$

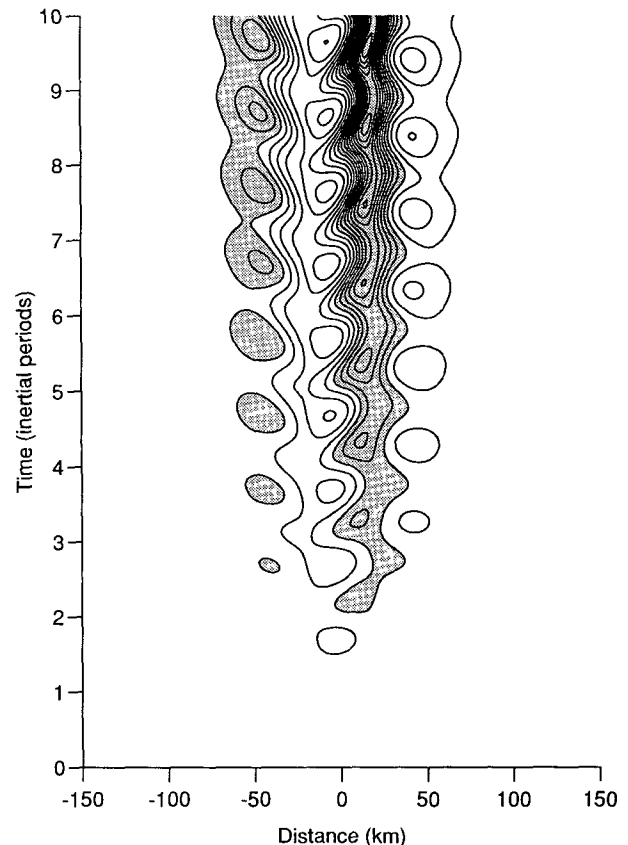


FIG. 2. As in Fig. 1 but for RR86's equations. Contour interval is 4 m, from -22 m to 50 m; positive values (downwelling) are shaded.

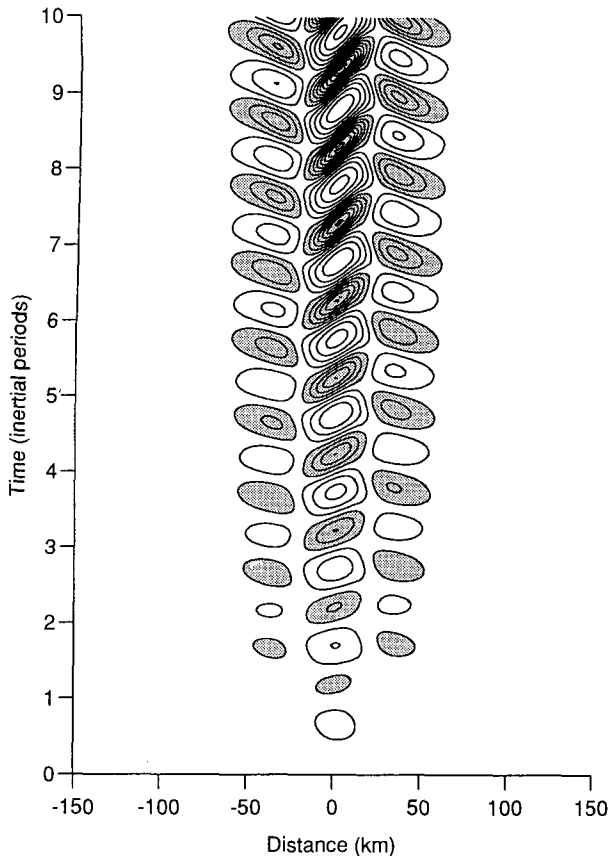


FIG. 3. As in Fig. 1 but for the nonlinear equations. Contour interval is 2 m, from -11 to 15 m; positive values (downwelling) are shaded.

$$\frac{\partial v^*}{\partial t^*} + \omega^2 u^* + \epsilon u^* \frac{\partial v^*}{\partial x^*} = 0$$

$$\frac{\partial h^*}{\partial t^*} + \epsilon \frac{\partial h^* u^*}{\partial x^*} = 0, \quad (7)$$

with $\omega^2(x) = 1 + \zeta(x)/f$. For any variable φ^* we use the following perturbation expansion in ϵ :

$$\varphi^* = \varphi_0^* + \epsilon \varphi_1^* + \epsilon^2 \varphi_2^* + \dots \quad (8)$$

with $\varphi^* = (u^*, v^*, h^*)$. The zeroth-order solution is

$$u_0^* = \frac{\sin(\omega t)}{\omega} \quad (9)$$

$$v_0^* = \cos(\omega t) \quad (10)$$

$$h_0^* = 1. \quad (11)$$

The higher-order variables are found by solving a sequence of linear systems forced by the nonlinear interactions of lower-order variables. Dropping asterisks for the sake of simplicity, h_1 is solution of

$$\frac{\partial h_1}{\partial t} = -\frac{\partial u_0}{\partial x}. \quad (12)$$

Taking into account the initial condition $h_1 = 0$, we obtain

$$h_1 = -\frac{t}{\omega^2} \frac{\partial \omega}{\partial x} \sin(\omega t) - 2 \frac{\partial \omega}{\partial x} \frac{(\cos(\omega t) - 1)}{\omega^3}. \quad (13)$$

This solution for h_1 is similar to KT93's solution for the linear system. The first term on the rhs of (13) is dominant for times longer than one inertial period. It represents a succession of upwellings and downwellings with an amplitude increasing with time and modulated by $\partial \omega / \partial x$, that is, by the vorticity gradient of the jet $\partial \zeta / \partial x$ (Fig. 1).

The zonal velocity u_1 is

$$u_1 = \frac{t}{2\omega^3} \frac{\partial \omega}{\partial x} (1 + \cos(2\omega t)) + \text{other oscillatory terms}, \quad (14)$$

where other oscillatory terms are the ones that do not involve t as a factor. Equation (14) shows that the velocity component u_1 has a nonoscillatory part, proportional to t , that comes from the nonlinear interaction $u_0 \partial v_0 / \partial x$. More precisely, the linear growth in t in (14) results from the equilibrium

$$\omega^2 u_1 \approx -u_0 \frac{\partial v_0}{\partial x}. \quad (15)$$

Note that in the case of RR86's equations, u_1 and v_1 are identically zero since the advection of momentum is neglected.

To the next order in ϵ , h_2 is solution of

$$\frac{\partial h_2}{\partial t} = -\frac{\partial h_1 u_0}{\partial x} - \frac{\partial u_1}{\partial x}. \quad (16)$$

Both terms on the rhs include a nonoscillatory part that is proportional to t :

$$\frac{\partial h_1 u_0}{\partial x} = \frac{\partial}{\partial x} \left(-\frac{t}{2\omega^3} \frac{\partial \omega}{\partial x} \right) + \text{oscillatory terms}$$

$$\frac{\partial u_1}{\partial x} = \frac{\partial}{\partial x} \left(\frac{t}{2\omega^3} \frac{\partial \omega}{\partial x} \right) + \text{oscillatory terms}.$$

It is readily seen that the nonoscillatory terms cancel each other. This effect can also be shown by writing the product $h_1 u_0$ as a function of v_0 using (9), (10), and (13):

$$h_1 u_0 = \frac{u_0}{\omega^2} \frac{\partial v_0}{\partial x} + 2u_0 \frac{(1 - v_0)}{\omega^3} \frac{\partial \omega}{\partial x}. \quad (17)$$

The first term on the rhs has a nonoscillatory part, which cancels the nonoscillatory part of u_1 as seen from (15).

Because of this cancellation between nonlinear effects the rhs of (16) is oscillatory, and the solution h_2 has the same characteristics as the linear solution h_1 , namely, oscillations proportional to the jet vorticity

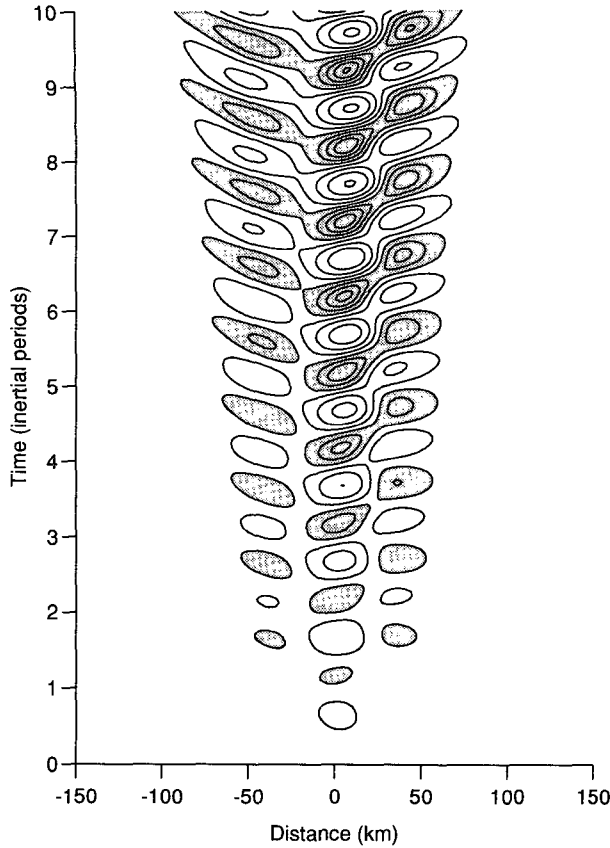


FIG. 4. Time-longitude plot of the mixed-layer depth perturbation for the nonlinear equations, with $g' = 2 \cdot 10^{-3} \text{ m s}^{-2}$ and $\nu = 10 \text{ m}^2 \text{ s}^{-1}$. Contour interval is 2 m, from -7 to 9 m; positive values (downwelling) are shaded.

gradient with an amplitude growing in time. This result agrees with the numerical experiments, which show no dramatic difference between the linear solution (Fig. 1) and the nonlinear solution (Fig. 3).

On the other hand, for the equations of RR86 that imply $u_1 = 0$, the nonoscillatory contribution from $\partial h_1 u_0 / \partial x$ does not cancel out and the leading term of the solution for h_2 is

$$h_2 \approx \frac{t^2}{4\omega^3} \left[\frac{\partial^2 \omega}{\partial x^2} - \frac{3}{\omega} \left(\frac{\partial \omega}{\partial x} \right)^2 \right] + \dots \quad (18)$$

The systematic growth or decrease of the mixed layer depth is modulated by $\partial^2 \omega / \partial x^2$ (this term is larger than $(\partial \omega / \partial x)^2$ when ζ / f is small, which is the case in RR86's and our experiments). Since ζ and $\partial^2 \omega / \partial x^2$ have similar structure with opposite signs, there is downwelling where the vorticity is negative and upwelling where the vorticity is positive. Those effects increase as t^2 and dominate the $O(\epsilon)$ term h_1 after some time. This explains the strongly asymmetric solution of RR86 (Fig. 2).

Note that the asymptotic expansion is not uniform. This simple expansion is used here to illustrate how

the nonlinear terms tend to cancel each other. A better approximate solution can be found by perturbations of the frequency (Y. Desaubies, personal communication).

4. Discussion

We have revisited the dynamics of free inertial oscillations in the presence of a mesoscale jet. The linear and fully nonlinear solutions of the shallow-water equations present similar characteristics. In both cases, the mixed layer depth is oscillatory in time, and its spatial structure is related to the vorticity gradient of the jet. The asymmetric growth or decrease of the mixed layer depth found by RR86 results from a partial neglect of the nonlinear terms, which is not justified by the asymptotic analysis. The spurious upwelling and downwelling effects are especially dramatic in the absence of horizontal dispersion ($g' = 0$).

When horizontal dispersion is important, energy tends to concentrate in the negative vorticity region as shown, for example, by Kunze (1985) and RR86, and the mixed layer depth oscillations are amplified there

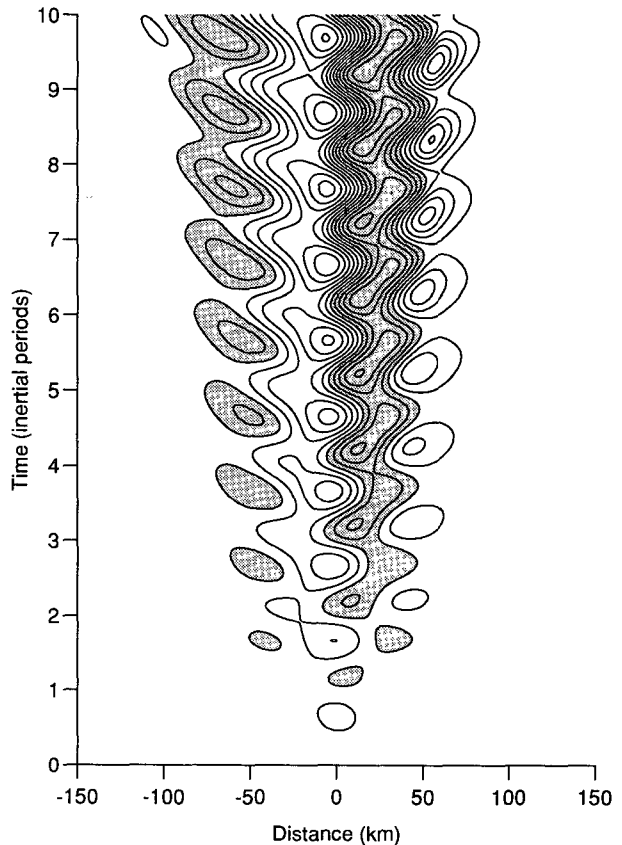


FIG. 5. Time-longitude plot of the mixed layer depth perturbation for RR86's equations, with $g' = 2 \cdot 10^{-3} \text{ m s}^{-2}$ and $\nu = 10 \text{ m}^2 \text{ s}^{-1}$. Contour interval is 2 m, from -13 to 11 m; positive values (downwelling) are shaded.

(Fig. 4). In that case, RR86's solution (Fig. 5) differs less from the fully nonlinear solution. Although a spurious systematic downwelling still occurs in the negative vorticity region, its maximum is only 40% higher than in the nonlinear solution of Fig. 4. (For the case $g' = 0$, there was a factor of 3 between downwellings in Figs. 2 and 3.) A similar decrease in amplitude is found between RR86's Figs. 3 ($g' = 0$) and 8 ($g' \neq 0$). Note that most results discussed by RR86 are obtained with a continuously stratified model where horizontal dispersion is taken into account and, therefore, should not depend much on the artifacts in the mixed layer depth response.

This example shows that when applying a shallow-water model to the dynamics of inertial oscillations, one should not neglect the nonlinear advection of momentum when the mass equation is nonlinear.

Editor's note: David Rubenstein replied to this comment as follows:

I agree with the comments of P. Klein and A. M. Tréguier. By including all of the nonlinear terms, they show that inertial oscillations in the vicinity of a front do not lead to systematic downwelling or upwelling of mixed layer depth. It is very interesting that the cross-frontal variations in mixed layer depth predicted by the fully nonlinear solution are comparable to those of the linear solution.

Acknowledgments. This work is supported by IFREMER and the CNRS. We thank J. P. Le Saos for helping us to run the first experiments.

REFERENCES

- Klein, P., and A. M. Treguier, 1993: Inertial resonance induced by a geostrophic jet. *J. Phys. Oceanogr.*, **23**, 1897–1915.
- Kunze, E., 1985: Near-inertial wave propagation in geostrophic shear. *J. Phys. Oceanogr.*, **15**, 544–565.
- , and T. B. Sanford, 1984: Observations of near-inertial waves in a front. *J. Phys. Oceanogr.*, **14**, 566–581.
- Niiler, P. P., 1969: On the Ekman divergence in an oceanic jet. *J. Geophys. Res.*, **74**, 28, 7048–7052.
- Rubenstein, D. M., and G. O. Roberts, 1986: Scattering of inertial waves by an ocean front. *J. Phys. Oceanogr.*, **16**, 121–131.